PNAS

Supporting Information for

Neuronal Innervation Regulates the Secretion of Neurotrophic Myokines and Exosomes from Skeletal Muscle

Kai-Yu Huang[1], Gaurav Upadhyay[2], Yujin Ahn[1], Masa Sakakura[3], Gelson J. Pagan-Diaz[4], Younghak Cho[5], Amanda C. Weiss[6], Chen Huang[7], Jennifer W. Mitchell[8], Jiahui Li[9], Yanqi Tan[7], Yu-Heng Deng[1], Austin Ellis-Mohr[3], Zhi Dou[2], Xiaotain Zhang[2], Sehong Kang[2], Qian Chen[9], Jonathan V. Sweedler[7], Sung Gap Im[5], Rashid Bashir[4], Hee Jung Chung[6], Gabriel Popescu[3], Martha U Gillette[8], Mattia Gazzola[2, 10], Hyunjoon Kong[1, 10, 11]*

[1] Department of Chemical and Biomolecular Engineering, University of Illinois at Urbana-Champaign, Urbana, Illinois 61801, USA

[2] Department of Mechanical Science and Engineering, University of Illinois at Urbana-Champaign, Urbana, Illinois 61801, USA

[3] Department of Electrical and Computer Engineering, University of Illinois, Urbana-Champaign, United States

[4] Department of Bioengineering, University of Illinois at Urbana-Champaign, Urbana, IL 61801, USA

[5] Department of Chemical and Biomolecular Engineering and KI for the Nano Century, Korea Advanced Institute of Science and Technology (KAIST), Daejeon 305-701, Republic of Korea

[6] Department of Molecular and Integrative Physiology, University of Illinois at Urbana-Champaign, Urbana, IL 61801, USA

[7] Department of Chemistry, University of Illinois at Urbana-Champaign, Urbana, IL 61801, USA

[8] Department of Cell and Developmental Biology, University of Illinois at Urbana-Champaign, Urbana, IL 61801, USA

[9] Department of Materials Science and Engineering, University of Illinois at Urbana-Champaign, Urbana, IL 61801, USA

[10] Carl R. Woese Institute for Genomic Biology, University of Illinois at Urbana-Champaign, Urbana, IL, USA

[11] KU-KIST Graduate School of Converging Science and Technology Korea University, Seoul, South Korea

*Corresponding author

Hyunjoon Kong, Ph.D.

Robert W. Schafer Professor

Department of Chemical and Biomolecular Engineering

University of Illinois at Urbana-Champaign

Urbana, IL 61801-3602

E-mail: hjkong06@illinois.edu

This PDF file includes:

Materials and Method

Figures S1 to S11

Tables S1

Legends for Movies S1 to S3

Legends for Datasets S1

Other supporting materials for this manuscript include the following:

Movies S1 to S3

Datasets S1

Materials and Method

Fabrication of patterned substrate

The polyurethane acrylate (PUA) substrates were fabricated using capillary force lithography.(1) The grooved PUA substrate was prepared by drop-dispensing PUA resins (MINS-311RM, Minuta Tech) on Si master with a grooved pattern (width = 1600 nm), subsequently covered with PET film (Skyrol, SKC Co.), and then exposed to ultraviolet light at 20 mW cm^{-2} for 10 s in the UV curing system (Minuta Tech, Korea). After initial UV cures, the PET film with the patterned PUA was detached from the Si mold and stabilized overnight. The flat substrate was fabricated by dropping the PUA resins on a flat Si surface in the same curing manner. All substrates were cleaned with isopropyl alcohol and distilled water for 30 minutes each. The morphology analysis of the PUA substrate was conducted using a scanning electron microscope (Hitachi S-4800).

Primary myoblast isolation

Primary myoblasts were harvested from an 8-week-old mouse (022CD1, Charles River). The isolation procedure followed the previous report(2). Briefly, muscle tissues collected from quadriceps, gastrocnemius, and soleus were sterilized with phosphate buffer saline (PBS) containing 40μg/mL gentamicin. All procedures were approved by the Institutional Animal Care and Use Committee (IACUC) at the University of Illinois at Urbana-Champaign in compliance with the National Institutes of Health Guide for the Care and Use of Laboratory Animals. The muscle fragments were plated on Matrigel (0.2 mg/mL) and collagen (0.2 mg/mL)-coated plate with media consisting of 40% v/v fetal bovine serum (FBS) and 10% v/v AmnioMAX C-100 supplement (Gibco) in DMEM/F12 for 5 days. The cells were detached with a trypsin-PBS mixture to harvest the outgrowing myoblast from the tissues and spun down at 200g for 5 minutes. Harvested cells were plated in Matrigel and collagen-coated T25 flask with myoblast media composed of 20% v/v FBS and 10% v/v amniotic fluid medium supplement in DMEM/F12 for proliferation. Once the cells reached 50% confluency, cells were detached from the flask. Cells were spun down at 200 g for 5 minutes, resuspended with myoblast media, and then seeded in a pre-coated T75 flask. 2 days later; the cells were passaged with PBS one more time to purify the cells further.

Primary hippocampal neurons isolation

Hippocampi were dissected in Hibernate-A (Brain Bits) from Long-Evans BluGill rats at Postnatal day 2 and chemically dissociated in Papain (Sigma-Aldrich, 18 Units/mL) for 30 minutes at 37˚C. The cells were then washed twice with Hibernate-A and mechanically dissociated through trituration with a glass pipette. After centrifugation, the neurons were resuspended in the growth medium, consisting of Neurobasal-A (Gibco), B27 Plus (Gibco, 2% v/v), GlutaMAX (Gibco, 1% v/v), and Penicillin-Streptomycin (Gibco, 1% v/v). All experiments were approved by the IACUC at the University of Illinois at Urbana-Champaign in compliance with the National Institutes of Health Guide for the Care and Use of Laboratory Animals.

Cellular orientation analysis

Bright field images of myotubes, on either flat or grooved substrates, were taken with an inverted microscope (LEICA DMi1) after 7 days of differentiation. Cellular orientation was analyzed by using the Directionality plugin in ImageJ. The direction was presented with the histogram showing the magnitude of cellular orientation from 0° to 180° counterclockwise. A Gaussian fitting was applied to the highest peak with the periodic nature of the histogram. ‘’Direction’’ and ‘’Dispersion’’ generated by the plugin represented the center of the Gaussian and the standard deviation, respectively. The R^2 values represented the goodness of fit.

Analysis of muscle contraction

Analysis of overall contracting area and contraction frequency

The contraction of skeletal muscle was quantified through custom MATLAB scripts. Frames were divided into sub-frames, each containing a single boundary of myotubes. A tracking function detected the movement of the boundary. Each deflection was counted as a contraction in the form of the peak for downstream analysis. The peak amplitude was not considered. The peak number divided by the total recording time was used to determine the average contraction rate mapped to the corresponding subframe. Peak trains were summed across all subframes to represent the overall contractions.

Visualization of localized muscle contraction in videos

A visualization algorithm based on the structural similarity (SSIM) index was developed to analyze muscle contraction.(3) 250 images (1024 × 768 pixels), captured at 25 frames/s, were extracted and divided into small patches (8 × 8 pixels) to analyze localized morphological changes between images. A total of 128 × 96 patches were generated in a single image. The localized SSIM index was then calculated by comparing the patches at the same coordinate in each image. The localized SSIM index was calibrated to the pixel intensity and associated with color maps to visualize muscle contraction. (Movie S1&S2)

Direction of muscle contraction analysis

Based on the SSIM index, the direction of muscle contraction was analyzed with the SSIM index arrays to generate a cumulative contraction map with a white area where significant localized contraction occurred and a black area corresponding to no contraction. Then, we obtained the numerical gradient between the white and black spots in the cumulative contraction map and analyzed the direction of muscle contraction using the vectors of the numerical gradient.

Contraction displacement

A low SSIM index means lots of structural change between each image; thus, the smaller localized SSIM number indicates greater contraction displacement. A rectangular area containing about 60 patches was segmented, and the normalized SSIM index was calculated to compare the muscle displacement between each experimental condition using the mean localized SSIM index from the segmented area.

Exosome analysis

After 8 days of co-culture, the cells were incubated with co-culture medium without horse serum for 24 hours. The supernatant was collected, and the exosomes were isolated with a total exosome isolation reagent (Invitrogen) following the manufacturer's instruction. Post incubation, the samples were centrifuged at 10,000g for 1 hour at 4°C. The supernatant was discarded, and the exosomes were resuspended with the cell culture medium. The exosome concentration was determined with NanoSight NS300 (Malvern Instruments). The exosome morphology was examined by transmission electron microscopy (JEOL 2100 Cryo TEM).

The total exosome RNA was extracted with Total Exosome RNA & Protein Isolation Kit (Invitrogen) following the manufacturer's protocol. From each culture, 1 mL of conditioned media containing between 10^7 and 10^8 exosomes was collected. Exosomes from 5 mL of conditioned media, representing five individual cultures, were combined to form one sample for RNA extraction. The purified RNA was then eluted in 60 μL of elution buffer. For each culture condition, three replicates were processed. The RNA libraries were prepared using the Qiaseq miRNA Library kit (Qiagen). Libraries were constructed using an EpMotion 5075 liquid handler (Eppendorf). Libraries were pooled in equimolar concentration. The pooled barcoded shotgun libraries were loaded on a NovaSeq lane for cluster formation and sequencing with NovaSeq 6000 Sequencing System (Illumina, San Diego, CA). The fastq read files were generated and demultiplexed with the bcl2fastq v2.20 Conversion Software. The miRNA mapping and quantification were performed by miRDeep2.(4) Differential expression of miRNA was analyzed with limma.(5) miRNA-target gene network, biological process enrichment analysis, and KEGG enrichment analysis were conducted in miRNet.(6)

To detect desmin protein in exosomes via LC-MS, exosomes were isolated from conditioned media using sequential ultracentrifugation. The conditioned media were first centrifuged at 300g for 5 minutes at 4°C to pellet cells, followed by a spin at 3000g for 20 minutes at 4°C to clear cellular debris, and finally ultracentrifuged at 100,000g for 2 hours at 4°C to precipitate exosomes. A volume of 5 mL of conditioned media was processed for each sample. Exosome samples of neuron-free muscle, innervated muscle, and neuron (n=4) were lysed using the Perfect-FOCUS kit (G-Biosciences). Post-protein extraction, samples underwent drying, reconstitution in 6M urea/50 mm NH_4HCO_3, and sequentially treated with DTT and iodoacetamide. After appropriate incubation and dilution steps, trypsin digestion was carried out at a 1:20 enzyme-to-protein ratio for 16 hours at 37°C. The dried protein digests were reconstituted in 200 μL of 0.1% formic acid in water and desalted using Pierce Peptide Desalting Spin Columns (ThermoFisher Scientific) following the manufacturer's instructions. The tryptic peptides were eluted with 600 μL of acetonitrile/water/FA (50/49.9/0.1), then dried completely in speed vac and stored at −80°C. Liquid chromatography (LC) separation of the tryptic peptides was performed on a nanoElute LC system (Bruker Daltonics) with a pre-concentration setup. Mobile phases consisted of LC–MS-grade water containing 0.1%

formic acid (solvent A) and LC–MS grade acetonitrile containing 0.1% formic acid (solvent B). The peptides were then separated on a nanoElue FIFTEEN column (Bruker Daltonics, 75 μm × 150 mm, C18, 1.9 μm particles, 120 Å pore size). The separation was carried out at 40°C with a flow rate of 400 nL/min using the following gradient: 2–10% B from 0 to 3 min, 10–40% B from 2 to 50 min, followed by a wash at 90% B for 7 min. The LC was coupled to a timsTOF Pro mass spectrometer (Bruker Daltonics) with a CaptiveSpray ion source, operating in parallel accumulation-serial fragmentation (PASEF) mode with TIMS activated and dynamic exclusion, 10 PASEF mass spectrometer / mass spectrometer scans per 1.1 s cycle. Raw data from each LC-TIMS-MS run were processed in PEAKS Online X (Bioinformatics Solutions Inc., Waterloo, ON) for peptide sequencing and protein identification. The information on mouse desmin from a *Mus musculus* protein database was sourced from UniProt. The search parameters set included a precursor mass error tolerance of 20 ppm and a fragment mass error tolerance of 0.05 . Carbamidomethylation of cysteine residues was set as a fixed modification and oxidation of methionine residues was set as a variable modification. Search result filters were set to a peptide FDR of 1% and a protein filter was set to a $-10\log P$ value ≥ 20.

Measurement of glutamic acid in conditioned media

Conditioned medium was collected on day 8 after 24 h of co-culture to analyze the remaining glutamic acid in the medium. The glutamic acid standard (part # 49449) was obtained from Sigma-Aldrich, and isotopically labeled standards (1,1,2,2-D_4 dopamine and AABB-D_4 serotonin) were obtained from Cambridge Isotope Laboratories. Isopropanol, methanol, water, and acetonitrile were LC-MS grade and obtained from Fisher Chemical. The extraction solution was made with 50/50 methanol/water (vol/vol). The background electrolyte solution for the microfluidic capillary electrophoresis (CE) device (ZipChip, 908 Devices) was prepared by mixing 1:25 metabolite acid: metabolite background electrolyte. Metabolite diluent was prepared by mixing 1:25 metabolite acid: metabolite diluent (908 Devices). A 10 mM glutamic acid standard was made by dissolving solid glutamic acid in water. Serial dilution was performed for subsequent concentrations needed for calibration by diluting the original stock with metabolite diluent with 1 μM of D4-isotopically-labeled serotonin as injection standard. D4-labeled dopamine standard was made by dissolving solid dopamine into the water to a final concentration of 10 mM.

Samples were thawed and vortexed to ensure proper mixing. 100 µL of each sample was aliquoted into a new sample tube, and the isotopically labeled dopamine standard was added to account for sample recovery. 100 µL of extraction solution was added to each sample, and samples were vortexed and sonicated for 5 min. After centrifuging at 14000 g for 15 min, the supernatant was collected and placed into a SpeedVac to remove excess moisture. Once dried, samples were stored in a -80° C freezer overnight before analysis.

CE analysis used a ZipChip interfaced to a Q-TOF electrospray mass spectrometer (ESI-MS) (maXis 4G, Bruker) using their high-speed microfluidic chip (908 Devices). This set up was adapted from the previous setup where amino acids and neurotransmitters were analyzed(7). Before attaching the ZipChip interface, Q-TOF ESI-MS was calibrated by directly infusing 10 mM sodium formate with an ESI source in the 70-1000 m/z mass range. Dried samples were reconstituted in a 1 µM D4-labeled serotonin internal standard solution made with metabolite diluent solution (908 Devices). Samples were analyzed in triplicates, and negative controls from all solutions used were analyzed to confirm no contamination. The field strength was set at 1000 V/cm, the run time for a single analysis was set at 3 min, and the injection volume was set at 20 nL. Data were analyzed using Compass Data Analysis 4.4 (Bruker). Extracted ion chromatograms were smoothed with the Gaussian smoothing function. m/z ratio and migration time of standards and samples were used to identify analytes. All peaks were integrated manually and normalized to the injection standard (D4-serotonin). Peaks were quantified with the calibration curve made at the beginning of the analysis that covered the expected concentration range.

MEA data processing

The raw data were first filtered using a standard fifth-order bandpass filtering of 300-3000 Hz. The filtered signal was then used to identify the spikes or action potentials by registering events when the voltage exceeded 5 times the signal noise estimate.(8) The obtained spike train information was used to calculate various spike rate (spikes/sec) based statistics such as the mean firing rate (firing rates across all electrodes/total number of electrodes), maximum firing rate (maximum spike rate across all electrodes), percentage of active electrodes (electrodes with firing rate > 0.2 spikes/sec). The spike train was further converted into a binned spike train with a bin size of 2 ms to estimate the pairwise Pearson correlation coefficient between the electrodes on different days.(9)

Figures

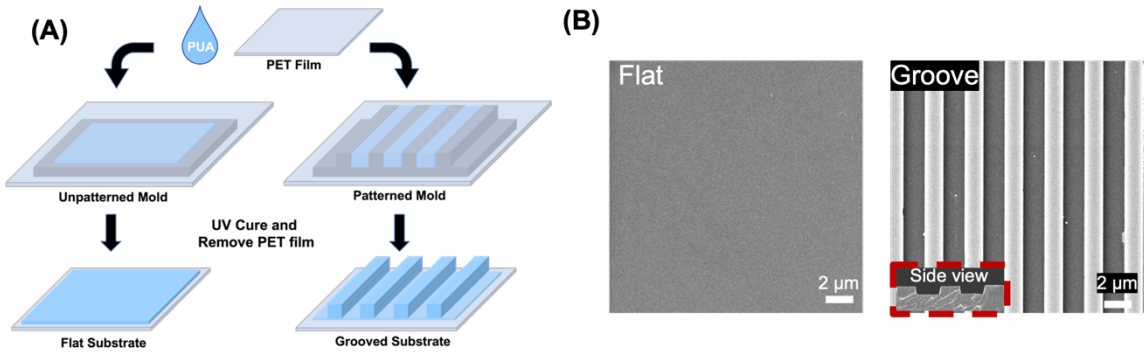

Figure S1. Fabrication process and analysis of polyurethane acrylate (PUA) substrates. (A) Schematic illustrating the fabrication procedure of the flat and micro-grooved substrates. (B) Scanning microscope (SEM) images of the PUA substrates with flat (left) and micro-grooved (right) topology.

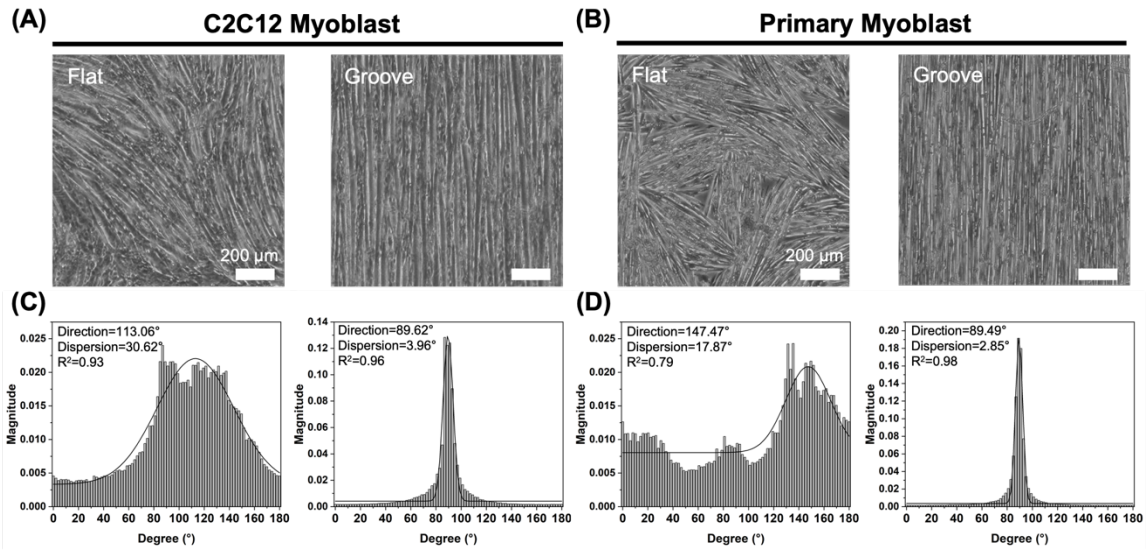

Figure S2. Angular orientation analysis of the engineered skeletal myotube. Optical images of (A) C2C12 myoblast-derived myotubes and (B) primary myoblast-derived myotubes on the flat and the micro-grooved (Groove) substrates. Images were captured after 7 days of myogenic differentiation. Representative histograms of the orientation of (C) C2C12 myoblast-derived and (D) primary myoblast-derived myotubes on the flat and the micro-grooved substrates. R^2 indicated the goodness of fit.

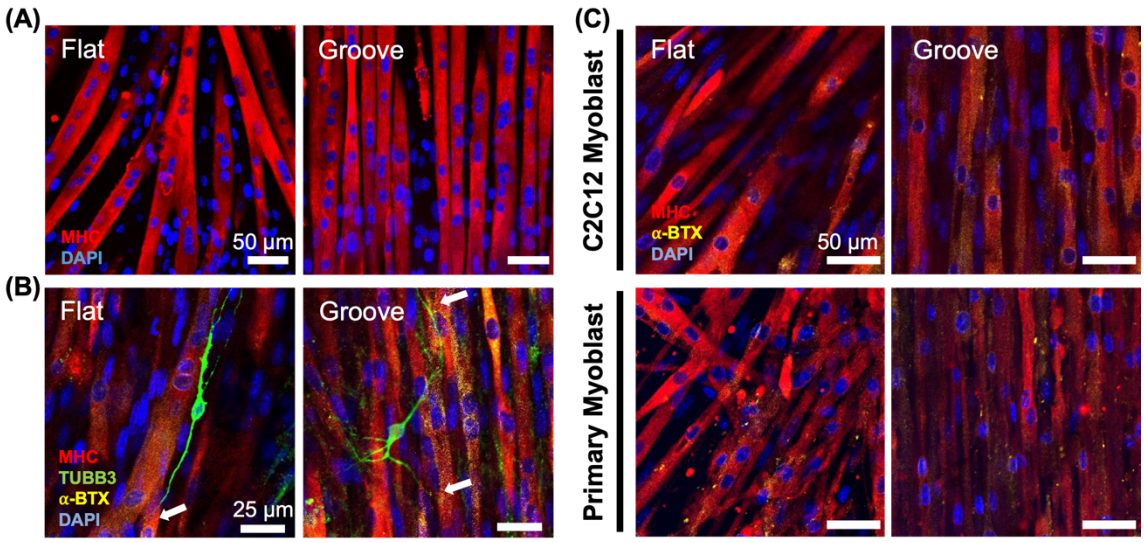

Figure S3. (A) Immunofluorescence images of myotubes (MHC, red) and nucleus (DAPI, blue) of C2C12 myoblasts differentiated on flat and micro-grooved (Groove) substrates. (B) Immunofluorescence images of neuron-innervated muscle made with C2C12 myoblasts cultured on a flat or a micro-grooved (Groove) substrate. [myotubes (MHC, red), neurons (TUBB3, green), AChRs (α-BTX, yellow), nuclei (DAPI, blue)] The white arrows indicated the innervation between the axonal terminal and clusters of AChRs. (C) Immunofluorescence images of clusters of AChR on neuron-innervated muscle after 8 days of coculture. [myotubes (MHC, red), AChRs (α-BTX, yellow), nuclei (DAPI, blue)]

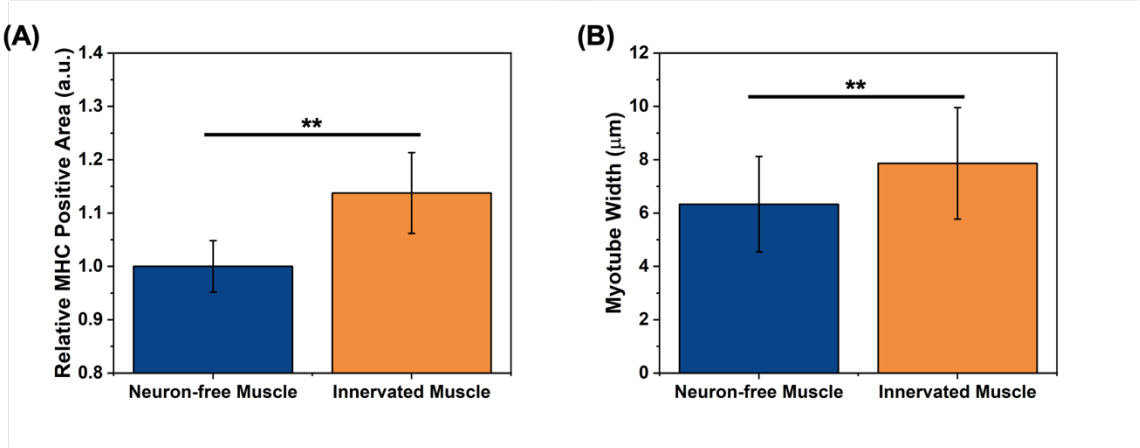

Figure S4. Effects of neuronal innervation on muscle growth. (A)The relative MHC positive area of neuron-free muscle and neuron-innervated muscle (Innervated Muscle). (n = 5, * = $p < 0.05$, ** = $p < 0.01$) (B) Width of myotubes of neuron-free muscle and Innervated Muscle. (n= 15, * = $p < 0.05$, ** = $p < 0.01$).

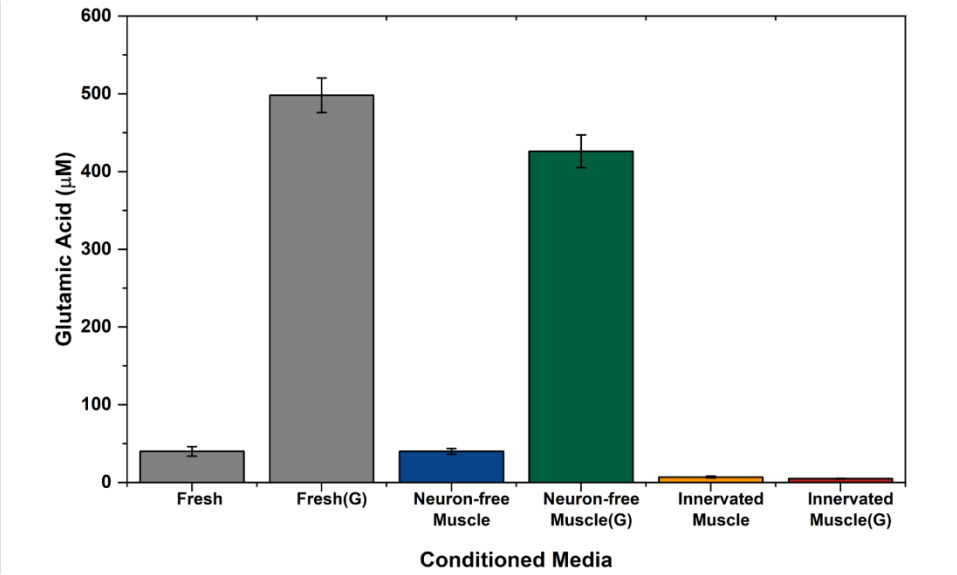

Figure S5. Glutamic acid concentration examined by Q-TOF ESI-MS of fresh cultured medium (Fresh), fresh cultured medium with 500μM glutamate addition [Fresh(G)], and conditioned media from neuron-free muscle (Neuron-free Muscle), neuron-free muscle with 500μM glutamate [Neuron-free Muscle(G)], neuron-innervated muscle (Innervated muscle), and neuron-innervated muscle with 500 μM glutamate [Innervated muscle(G)] after 24-hour incubation.

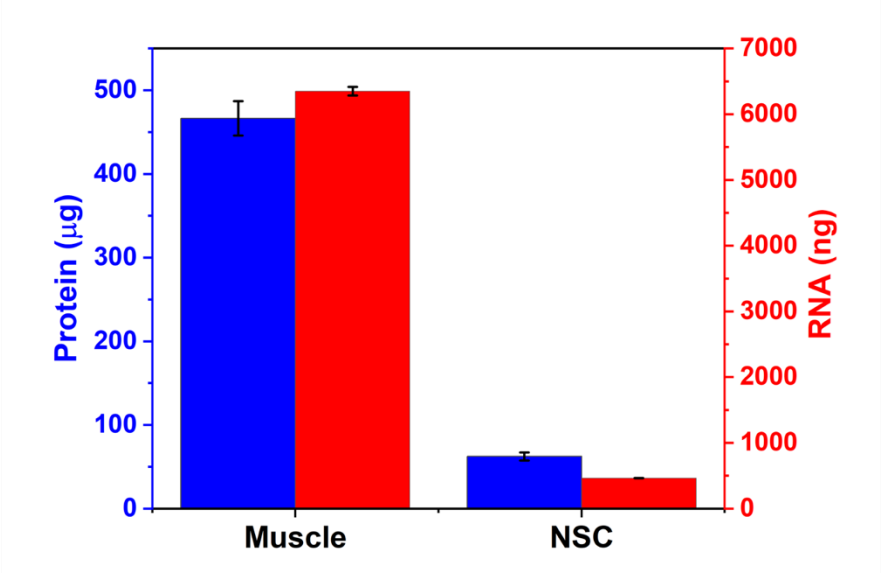

Figure S6. Total protein and RNA amounts of skeletal muscle cells and NSC cells used for co-culture.

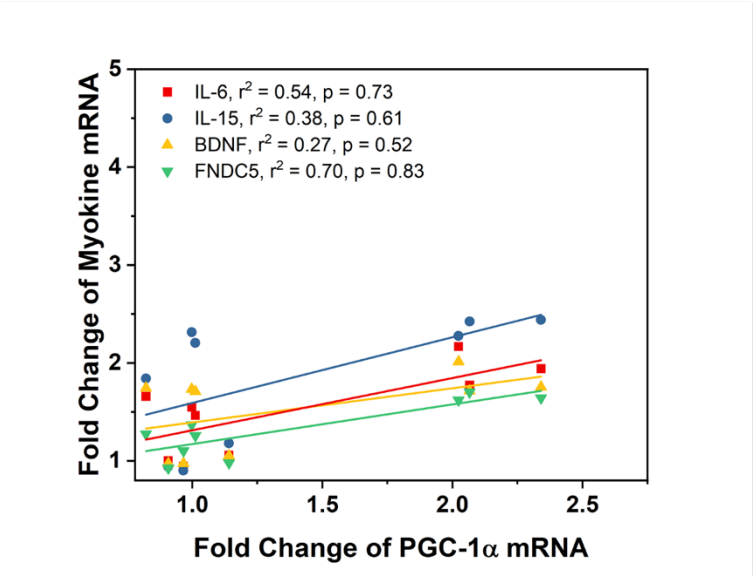

Figure S7. Correlation of IL-6, IL-15, BDNF, and FNDC5-encoding mRNA expressions to PGC-1α-encoding mRNA expression of the muscles on the flat substrates. (r2: R-squared value, p: correlation coefficient)

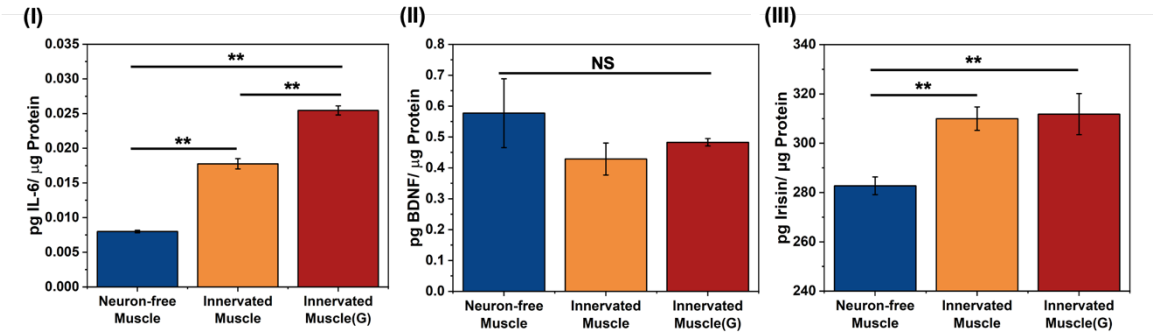

Figure S8. Effect of neuronal innervation on myokine production. Intracellular concentrations of (I) IL-6, (II) BDNF, and (III) Irisin of Neuron-free Muscle, Innervated Muscle, and Innervated Muscle(G), normalized to total intracellular protein measured after 8 days of co-culture. Primary myoblasts and NSCs were differentiated and co-cultured on the micro-grooved substrates. (n = 3, * = $p < 0.05$, ** = $p < 0.01$)

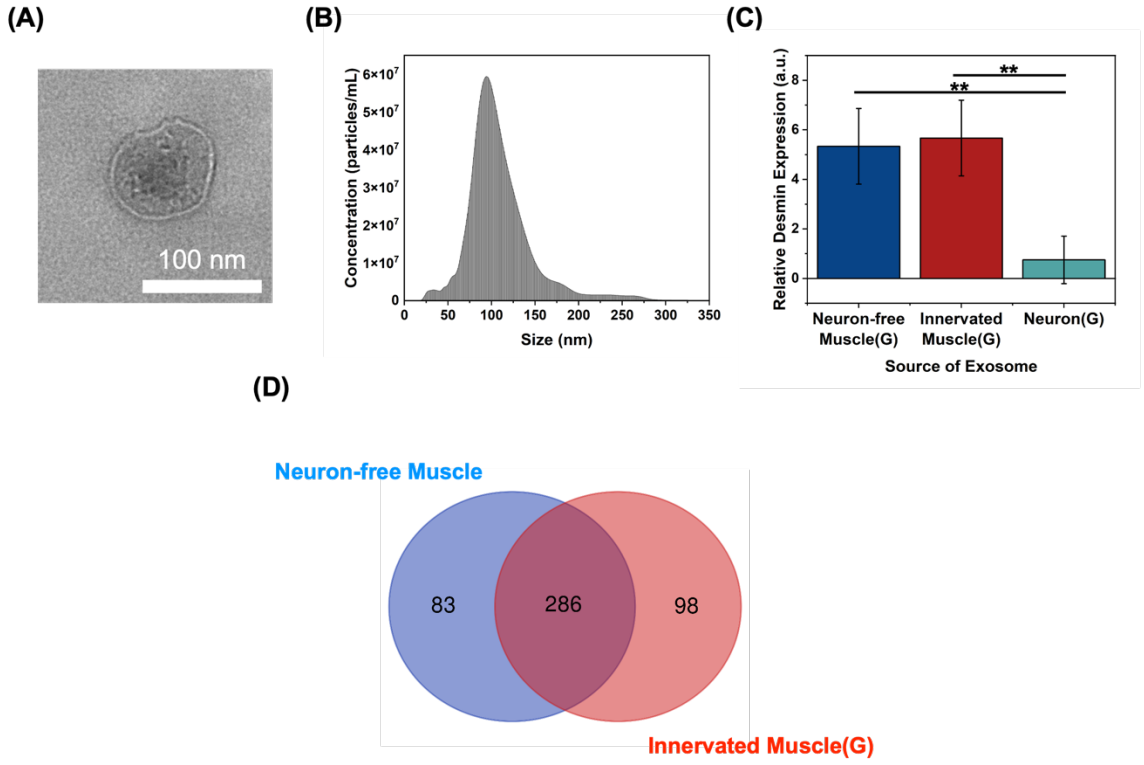

Figure S9. Exosome released from engineered muscle. (A) TEM images and (B) size distribution of exosomes isolated from the conditioned media of neuron-innervated muscle stimulated with glutamate. (C) Relative expression of desmin in the exosomes from neuron-free muscle [Neuron-free Muscle(G)], neuron-innerved muscle [Innervated Muscle(G)], and NSC-derived neurons [Neuron(G)]. All conditions were incubated with 500uM glutamate. (n = 3, * = $p < 0.05$, ** = $p < 0.01$) (D) Venn diagram showing the overlap of exosomal miRNA between Neuron-free muscle and Innervated Muscle(G).

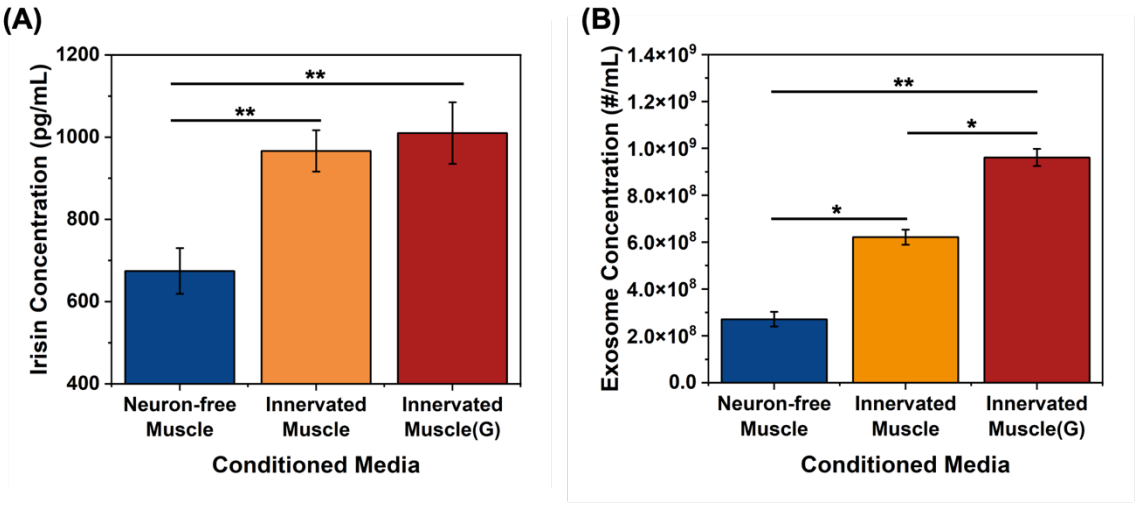

Figure S10. Concentrations of (A) irisin and (B) exosome in conditioned media harvested from Neuron-free Muscle, Innervated Muscle, and Innervated muscle(G) after 24-hour incubation. (n = 3, * = $p < 0.05$, ** = $p < 0.01$)

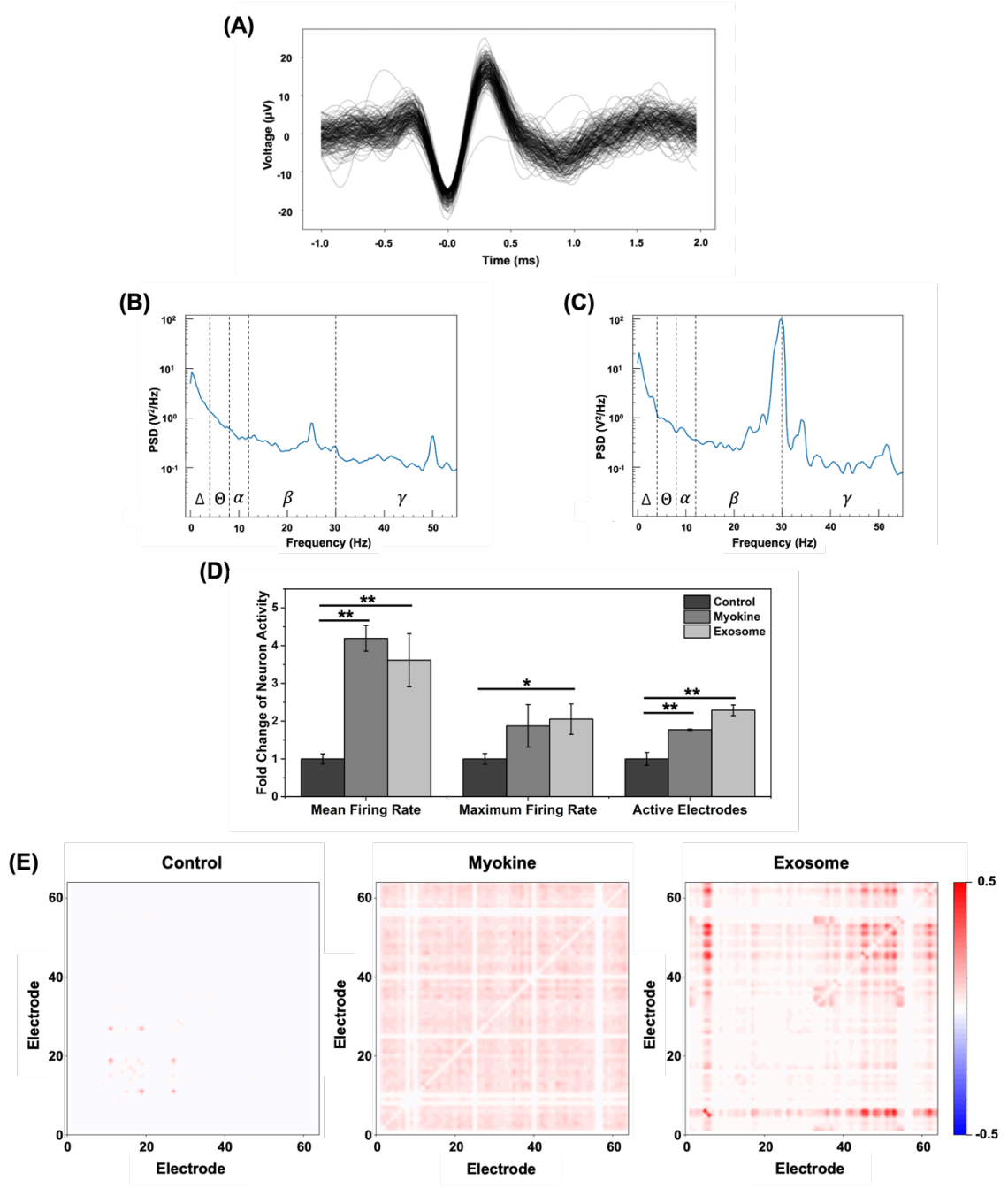

Figure S11. (A) Spike cutouts from one of the electrodes show the characteristic dip in the voltage, which is interpreted as a spike event. (B) Power spectra of the local field potential on electrodes with neurons incubated with Innervated Muscle(G) medium. (C) Power spectra of the local field potential on electrodes from neurons incubated with Neuron-free Muscle medium. (D) Relative change of mean firing rate, maximum firing rate, and active electrodes of primary hippocampal neurons cultured with purified proteins (Myokine) or exosomes (Exosome) in the Innervated Muscle(G) medium. Neurons were cultured with these

purified proteins (0.3 mg/mL) or exosomes (10^8 exosomes/mL) for 7 days. Each value was normalized to the control condition, which is neurons cultured without additives. (n = 3, * = $p < 0.05$, ** = $p < 0.01$) (E) Correlation between electrodes of neurons cultured on MEA without or with the addition of purified proteins or exosomes.

Table S1. Primer sequences used for RT-PCR analysis.

Target Gene	Forward Primer (5'-3')	Reverse Primer (5'-3')
GAPDH	CATCACTGCCACCCAGAAGACTG	ATGCCAGTGAGCTTCCCGTTCAG
PGC-1α	GAATCAAGCCACTACAGACAC CG	CATCCCTCTTGAGCCTTTCGTG
IL-6	TACCACTTCACAAGTCGGAGGC	CTGCAAGTGCATCATCGTTGTTC
IL-15	GTAGGTCTCCCTAAAACAGAGGC	TCCAGGAGAAAGCAGTTCATTGC
BDNF	GGCTGACACTTTTGAGCACGTC	CTCCAAAGGCACTTGACTGCTG
FNDC5	GATGTCCTGGAGGATGAAGTGG	GTGGTGGTGTTCACCTCCTGAA
ANK2	ATCGGAGTCAGATCAAGAGCCG	AAGCCAGCCTTTCTTCCATCCG
FGFR1	GCCTCACATTCAGTGGCTGAAG	AGCACCTCCATTTCCTTGTCGG
FOXG1	TACTACCGCGAGAACAAGCAGG	GAGCATCCAGTAGTTGCCCTTG
FOXP1	CATGCCTCTACCAATGGACAGC	GAAGTCGTCACAAACCGCCTCA
FOXP2	GCATTGGATGACCGAAGCACTG	TCGCATGTGCAAGTGGGTCATC
JAG1	TGCGTGGTCAATGGAGACTCCT	TCGCACCGATACCAGTTGTCTC
KIF1A	CGCTGACATCTTCTGCCAGTTC	CGATGAAGGACTTGGTCACCTC
PUM2	AAGTGCGTCTCTTGGCTGTGGA	GAGACTCTCTCCTTGTGGCACT
SIRT1	GGAGCAGATTAGTAAGCGGCTTG	GTTACTGCCACAGGAACTAGAGG
SYT1	AGTCTTCCTGCTGCCCGACAAA	CACAGCCATCACCAGTGTCTTG
CAMK2G	GGACACAGTCACTCCTGAAGCT	TCTACCGTCTCTTGGCGATGCA
EGR1	AGCGAACAACCCTATGAGCACC	ATGGGAGGCAACCGAGTCGTTT

Movie S1 (separate file). Contractions of muscle models created on flat substrates

Movie S2 (separate file). Contractions of muscle models created on micro-grooved substrates

Movie S3 (separate file). Axonal transports of primary hippocampal neurons cultured with conditioned medium

Dataset S1 (separate file). Total miRNA count, top95% miRNA and the target gene.

Reference

1. H. S. Yang *et al.*, Electroconductive Nanopatterned Substrates for Enhanced Myogenic Differentiation and Maturation. *Advanced Healthcare Materials* **5**, 137-145 (2016).
2. M. Au - Vaughan, K. A. Au - Lamia, Isolation and Differentiation of Primary Myoblasts from Mouse Skeletal Muscle Explants. *JoVE* doi:10.3791/60310, e60310 (2019).
3. W. Zhou, A. C. Bovik, H. R. Sheikh, E. P. Simoncelli, Image quality assessment: from error visibility to structural similarity. *IEEE Transactions on Image Processing* **13**, 600-612 (2004).
4. M. R. Friedländer, S. D. Mackowiak, N. Li, W. Chen, N. Rajewsky, miRDeep2 accurately identifies known and hundreds of novel microRNA genes in seven animal clades. *Nucleic Acids Research* **40**, 37-52 (2011).
5. M. E. Ritchie *et al.*, limma powers differential expression analyses for RNA-sequencing and microarray studies. *Nucleic Acids Research* **43**, e47-e47 (2015).
6. L. Chang, G. Zhou, O. Soufan, J. Xia, miRNet 2.0: network-based visual analytics for miRNA functional analysis and systems biology. *Nucleic Acids Research* **48**, W244-W251 (2020).
7. C. J. Lee *et al.*, d-Amino Acids and Classical Neurotransmitters in Healthy and Type 2 Diabetes-Affected Human Pancreatic Islets of Langerhans. *Metabolites* **12**, 799 (2022).
8. J. Joy, S. Peter, N. John, DENOISING USING SOFT THRESHOLDING. *International Journal of Advanced Research in Electrical, Electronics and Instrumentation Energy* **2**, 1027-1032 (2013).
9. C. S. Cutts, S. J. Eglen, Detecting pairwise correlations in spike trains: an objective comparison of methods and application to the study of retinal waves. *J Neurosci* **34**, 14288-14303 (2014).